APPLICATION OF INFRARED REFLECTANCE SPECTROSCOPY TO ELECTROCATALYSIS

C. LAMY, F. HAHN and B. BEDEN,

Laboratoire de Chimie I, UA au CNRS 350 "Catalyse en Chimie Organique", Université de Poitiers, 40, avenue du Recteur Pineau, 86022 POITIERS, France.

ABSTRACT

The application of Electro-Modulated Infrared Reflectance Spectroscopy (EMIRS) to electrocatalysis is illustrated by several typical examples such as the electrooxidation of formic acid at rhodium, the self-poisoning of platinum electrode, the elucidation of the electrocatalytic behaviour of polycrystalline platinum for the oxidation of methanol, the effect of Pb and Cd adatoms on the electrocatalytic activity of Rh electrodes for formic acid oxidation, and the adsorption of ethanol and of carbon dioxide at a platinum electrode.

RESUMO

A aplicação da Espectroscopia Infra-vermelho de Reflectância Electro-Modulada (EIREM) em electrocatálise é ilustrada com vários exemplos, tais como : a electro-oxidação do ácido fórmico sobre ródio, o auto-envenenamento dos electrodos de platina, a determinação do comportamento electrocatalitico da platina policristalina na oxidação do metanol, os efeitos dos ad-atomos de chumbo e de cádmio sobre a actividade electrocatalítica do ródio na oxidação do ácido fórmico e a adsorção do etanol e a electro-redução do dioxido de carbono sobre platina.

Plenary lecture held at the 4th Meeting of the Portuguese Electrochemical Society, Estoril, March 1989

Portugaliæ Electrochimica Acta, 7 (1989) 435-456

INTRODUCTION

Electrocatalysis can be defined as the heterogeneous catalysis by the electrode material of electrochemical reactions, i.e. electron transfer reactions occuring at the interface between an electronic conductor, the electrode, and an ionic conductor, the electrolyte [1]. Like in heterogeneous catalysis the reaction mechanism involves both mass transfer in the bulk of electrolyte, and surface reactions at the electrode-electrolyte interface, mainly adsorption and charge transfer. The kinetics of these surface reactions does not only depend on the interface area, but also on the electrode potential. An electrocatalytic reaction is therefore activated by a combination of the catalytic action of the electrode material, and of the activation effect of the interfacial electric field resulting from the applied potential, E. This leads to lower the potential barrier by an amount K arising from the presence of the catalyst and by a fraction αnFE of the electrical energy (Fig.1).

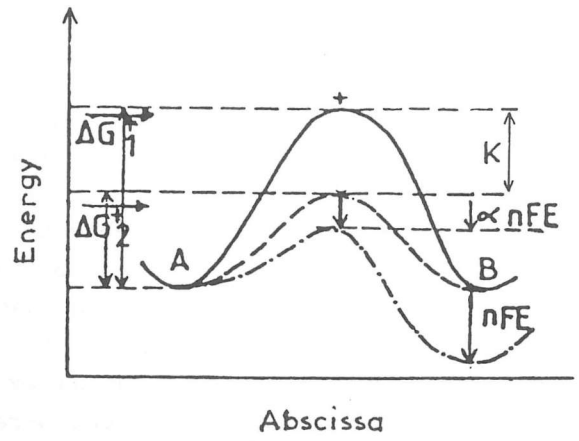

Figure 1 : Principle of electrocatalytic activation

Apart from the electrocatalytic oxidation of hydrogen, and the electrocatalytic reduction of oxygen, which have been widely studied, both from a fundamental

point of view, and for practical use in hydrogen/air fuel cells, or in water electrolysis[2], only a few other electrocatalytic reactions were considered involving different small organic molecules[3]. These reactions are much more complex since they involve a great number of transfered electrons and several reaction products and adsorbed species. Like in heterogeneous kinetics, the adsorbed intermediates play a key role in the overall reaction, as the more as they determine the reaction pathway (reactive intermediates), i.e. the reaction selectivity, and the electrocatalytic activity (poisoning intermediates). The goal for a detailed kinetic study on electrocatalytic reactions is therefore the identification of adsorbed intermediates, and the analysis of reaction products and byproducts. This can only be achieved by very powerful surface techniques and analytical techniques, which may work "in situ". In particular, "in situ" investigation of the electrode-electrolyte interface may be conveniently performed using reflectance spectroscopic methods, either in the UV-Visible range or in the Infrared range. These techniques are able to analyze the structure of the interface at the molecular level, even in the presence of strong absorbing media such as aqueous solutions. Specular reflection spectroscopy in the infrared range is particularly useful for identifying, by their vibrational fingerprints, the different species present at the electrode surface, such as chemisorbed intermediates resulting both from the dissociative adsorption of the electroactive species, and of the solvent (water in these studies).

This paper aims to show how Infrared Reflectance Spectroscopy is well adapted to the elucidation of reaction mechanisms of electrocatalytic reactions occuring in fuel cells or in electroorganic synthesis.

PRINCIPLES OF INFRARED REFLECTANCE SPECTROSCOPY

Infrared Reflectance Spectroscopy consists in illuminating, through a thin electrolyte layer, the electrode surface by an infrared beam. The reflected light, after its detection by a Mercury-Cadmium Telluride detector, is amplified by a synchronous detector, in order to improve the signal-to-noise ratio, which is otherwise very poor due to the weakness of the IR signal. This results both from strong absorption of the IR light by the electrolytic solution (aqueous solution) and from the small amount of absorbing species at the electrode surface, compared to those in the bulk electrolyte. For a complete monolayer, this corresponds to about 10^{15} adsorbed species per cm^2, which is very low, compared to about 10^{22} species per cm^3 of solution. A thin layer spectroelectrochemical cell adapted to aqueous solution was designed by Bewick et al.(4), and is shown in fig.2.

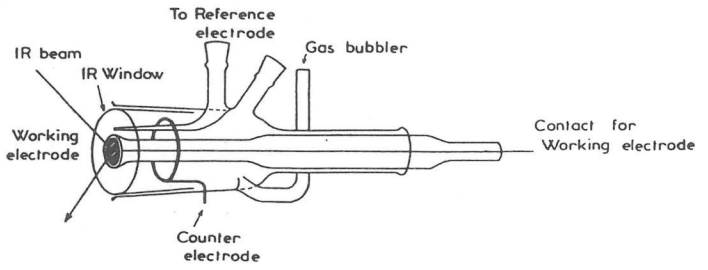

Figure 2 : Schematic diagram of the electrochemical cell used for external IR light reflection

The synchronous detection of the infrared signal is achieved by modulating the signal and using a lock-in amplifier, which discriminates the in-frequency and in-phase useful signal from background and noise. In the so-called "Electrochemically Modulated Infrared Reflectance Spectroscopy" (EMIRS), which is used in this work, the modulated infrared signal results from electrode potential modulation at a suitable amplitude (a few hundreds of mV),

and a given frequency (a few tens of Hz). This modulation signal, provided by a waveform generator, is added to the average electrode potential by means of a potentiostat, which allows a full control of the potential of the working electrode (WE), through the reference electrode (RE) and the counter electrode (CE). The signal detected at the output of the lock-in amplifier, which has very often a derivative-like shape, is further improved by signal averaging techniques, and then processed by means of a microcomputer system. The block diagram of the complete system is shown in Figure 3.

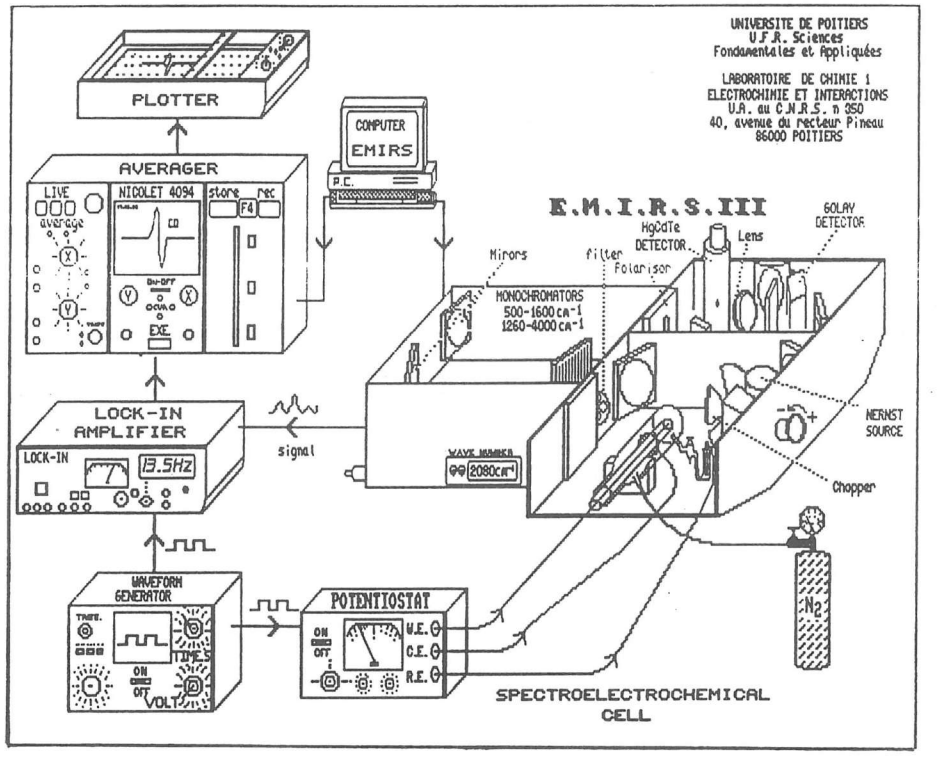

Figure 3 : Block diagram of the EMIRS system

This equipement allows us to monitor very small relative reflectivity changes, $\Delta R/R$, of the order of 10^{-4} to 10^{-5}, which are sufficient to observe submonolayers of adsorbed species on a small area ($\approx$ 0.5 cm^2) electrode

(e.g. a full monolayer of adsorbed CO, which is a strong IR absorber, gives $\Delta R/R \approx 10^{-3}$).

Other Infrared Reflectance Spectroscopic techniques, like Subtractively Normalized Interfacial Fourier Transform Infrared Spectroscopy (SNIFTIRS) using also potential modulation, and Infrared Reflection-Absorption Spectroscopy (IRRAS) using polarization modulation, are also suitable for investigating electrocatalytic problems, but they will not be described here (see e.g. ref.5).

APPLICATION OF EMIRS TO SELECTED EXAMPLES

The application of EMIRS to electrocatalysis will be illustrated by selected examples taken from our Laboratory. They will concern essentially the adsorption and the electrooxidation of small organic molecules, such as formic acid, methanol, ethanol,..., and also the electroreduction of carbon dioxide, on various catalytic electrode materials (Pt, Rh,...).

i) Mechanisms of the electrooxidation of formic acid at rhodium(6)(7). Effect of foreign metal adatoms(8)

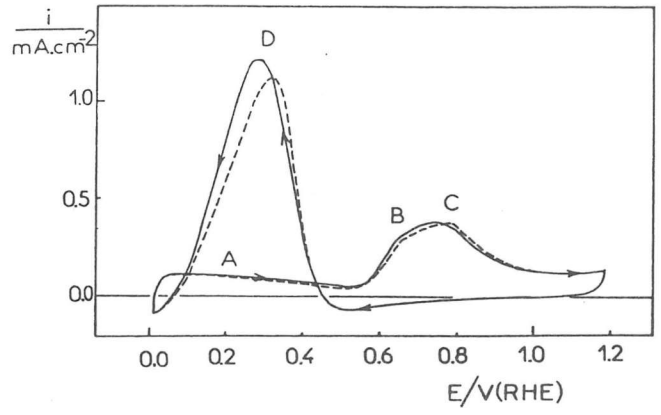

Figure 4 : Voltammograms recorded during the oxidation of 0.1 M HCOOH on Rh in 0.5 M $HClO_4$ (100 mV/s, 25°C). The curve in dashed line is obtained whith the electrode surface pushed against the cell window

The dissociative adsorption of formic acid at a rhodium electrode, in a potential range where no oxidation occurs (i.e. E < 0.6 V/RHE - see the voltammogram in figure 4), gives two derivative-like infrared bands (Fig.5b). By comparison with the EMIRS bands due to adsorbed CO species, resulting from adsorption of gaseous CO dissolved into the electrolytic solution, and recorded under the same experimental conditions (Fig.5a), these bands were assigned to linearly-bonded -CO (CO_L at around 2050 cm^{-1}) and to bridge-bonded >CO (CO_B at around 1925 cm^{-1}), respectively. The intensity of the IR band of CO obtained from HCOOH is comparable to that due to the species originated from dissolved CO, which adsorbs at nearly a full coverage of the electrode surface, as measured by an electrochemical method (cyclic voltammetry).

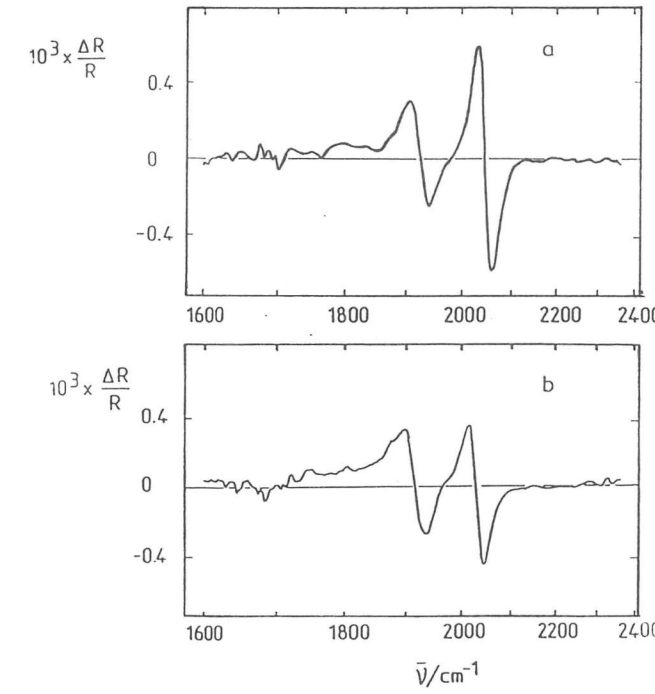

Figure 5 : EMIRS spectra of CO adsorbed on Rh in 0.25 M $HClO_4$ (ΔE = 0.4 V, f = 13.5 Hz) : a) CO from gaseous CO dissolved in the supporting electrolyte; b) CO from the chemisorption of 0.1 M HCOOH

However, the intensity ratio of the two CO bands is slightly different, with a smaller amount of linearly-bonded CO in the case of formic acid adsorption. This leaves the possibility that other species might be linearly-bonded to the rhodium surface. This is effectively verified, since another species is detected by a double band near 1360 and 1390 cm^{-1}, which is particularly visible in alkaline medium (Fig.6), for which the amount of linearly-bonded CO, which acts as a poisoning species, is smaller than in acid medium. These bands are assigned to adsorbed formate, by comparison with the corresponding bands for free formate in aqueous solution at 1335 and 1383 cm^{-1}. The small shift of the wavenumber of an adsorbed species compared to that of free species, is usually observed, because of modification of the bond strength due to interactions with the catalytic surface. An other relatively intense band is also seen at around 1325 cm^{-1}, which arises from adsorbed CO_2 , as discussed in the last section of this paper.

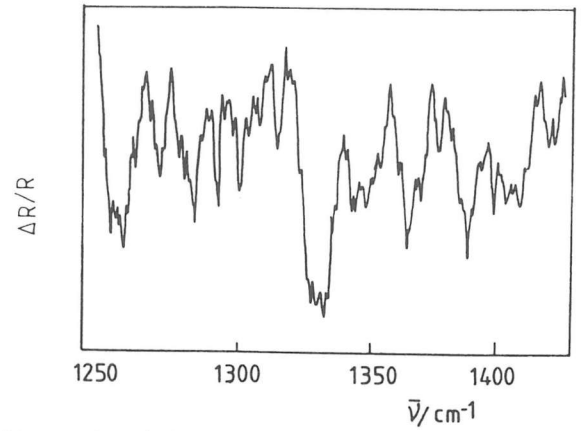

Figure 6 : EMIRS spectrum of adsorbed formate from 0.1 M HCOONa in 0.1 M NaOH (ΔE = 0.4 V, f = 13.5 Hz)

The effect of foreign metal adatoms (Bi, Cd, Pb, Tl,...) on the electrocatalytic activity of noble metal electrodes (Pt, Rh, Pd,...) is clearly illustrated in the case of the electrooxidation of formic acid at rhodium.

Adatom submonolayers are easily obtained by underpotential deposition, i.e. by electrodeposition of the metal adatoms at potentials more positive than the thermodynamic potential for bulk deposition. Some of these adatom layers are known to enhance greatly the electrocatalytic oxidation of small organic molecules [9].

The origin of this effect was not yet really elucidated: electronic factor, geometric factor, bifunctional theory of electrocatalysis, modification of the nature and distribution of adsorbed species. This effect is now better understood, as illustrated in the case of Pb and Cd adatoms modified Rh electrodes for the electrooxidation of formic acid [8].

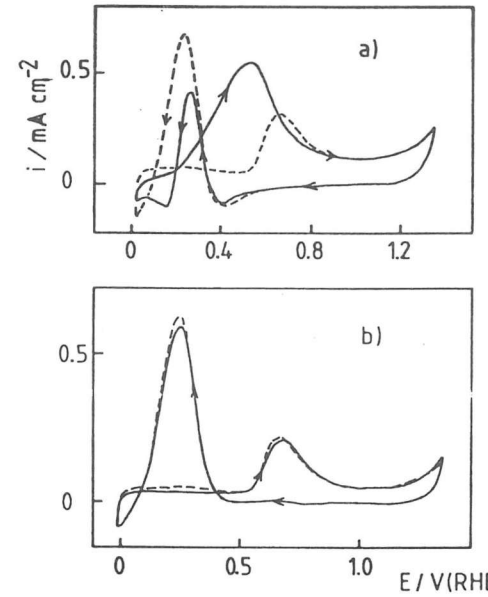

Figure 7 : Voltammograms showing the oxidation of 0.1 M HCOOH in 0.5 M $HClO_4$ on adatoms modified Rh electrodes. (50 mV/s, 25°C). The dashed curves correspond to unmodified Rh. a) Pb adatoms from $5x10^{-4}$ M Pb^{2+}; b) Cd adatoms from 10^{-3} M Cd^{2+}.

Lead adatoms can enhance the oxidation of formic acid, while Cd adatoms do not, as seen in the voltammograms of figure 7. It is as much surprising as the underpotential

deposition of both adatoms occurs in the same potential range, and as they lead to a similar decrease of the hydrogen adsorption region. Lead adatoms have a specific behaviour, since they affect only bridge-bonded CO, without affecting the other adsorbed species, when the bulk concentration of Pb^{2+} increases from 5.10^{-7} M to 10^{-3} M, as seen in the EMIRS spectra in fig.8. This leads to a one-by-one replacement of bridge-bonded CO by Pb adatoms, suggesting that lead adatoms occupy two adjacent adsorption sites.

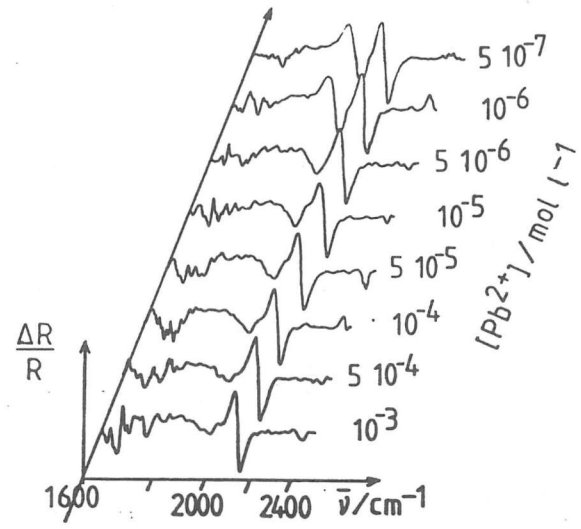

Figure 8 : EMIRS spectra of CO_{ads} resulting from the adsorption of 0.1M HCOOH in 0.5 M $HClO_4$ on Rh electrodes modified by lead adatoms recorded at various $C_{Pb^{2+}}$

Conversely, with Cd adatoms, no changes occur in the EMIRS spectra, until very high concentrations of the precursor salt are attained ($C_{Cd^{2+}} > 10^{-2}$ M). This is illustrated in figure 9, giving the dependence of the band intensities, for CO_L and CO_B, vs. the bulk concentration of the precursor salts (Pb^{2+} and Cd^{2+}).

These results show that Cd adatoms are more weakly adsorbed than lead adatoms, and that they cannot compete with CO adsorption to prevent its adsorption, thus explaining their lack of effect in the enhancement of

activity of rhodium for formic acid oxidation. At high concentrations of Cd^{2+}, some impurities, such as lead, may act as adatoms, and affect the electrocatalytic activity of rhodium.

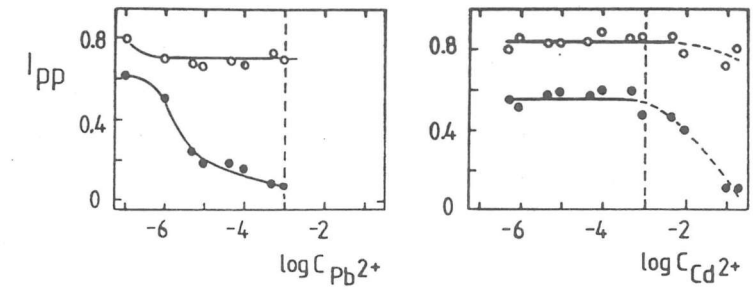

Figure 9 : Variation of the EMIRS bands intensities of CO_{ads} resulting from the adsorption of HCOOH at Rh modified by Pb and Cd adatoms (o: CO_L; ●: CO_B)

All these spectroscopic results allow us to suggest a reaction mechanism involving different adsorbed species, such as formate acting as a reactive intermediate, linearly-bonded CO_L and bridge-bonded CO_B acting as poisoning intermediates, together with superficial rhodium oxides formed at the anodic potentials where the oxidation of formic acid occurs, as evidenced by UV-Visible Reflectance Spectroscopy [10].

(ii) Elucidation of the electrocatalytic behaviour of platinum for the oxidation of methanol

Different mechanisms were suggested in the literature to explain the oxidation of methanol on platinum electrodes in acid medium [11]. Some of them involve ->COH, or -CHO, as reactive intermediates, and some others propose -CO as active adsorbed species. But surprisingly, none of them accounted clearly for the formation of catalytic poisons, nor for the role of the electrode structure. The first investigation of this problem by EMIRS, in 1981, showed unambiguously that the platinum electrode surface is covered by a large amount of adsorbed carbon monoxide as a result of methanol chemisorption[12]. It was recognized

that CO was mainly linearly-bonded to the surface (band at 2080 cm^{-1}), ant that another minor species was bridge-bonded CO (band at 1870 cm^{-1}). These results were later confirmed by numerous infrared spectroscopic studies, using EMIRS [13], Linear Potential Sweep Infrared Reflectance Spectroscopy (LIPSIRS) [14], or Subtractively Normalized Interfacial Fourier Transform Infrared Reflectance Spectroscopy (SNIFTIRS)[15].

Under usual experimental conditions (small surface area, relatively concentrated methanol solutions, long spectral acquisition times,...), adsorbed CO, particularly linearly-bonded CO_L, accumulates at the electrode surface, blocking progressively the electrode active sites, thus explaining the self-poisoning of platinum electrodes during methanol oxidation. In order to favour weakly adsorbed species, particularly linearly-bonded to the surface, such as -CHO or -COOH, experimental conditions were found, where the electrode coverage by the CO poisoning species can be greatly reduced. This is the case of electrolyte solutions with a low concentration of methanol[16], and also the case of rough platinum electrodes[17].

For a $5x10^{-3}$ M CH_3OH in 0.5 M $HClO_4$ solution, EMIRS spectra recorded at a smooth polycrystalline platinum electrode during the first stages of methanol adsorption (1^{st} unaveraged scan) clearly show several absorption bands in the spectral range 1300-3000 cm^{-1} (fig.10a). Apart from a very small band at 2050 cm^{-1} assigned to linearly-bonded CO, there are a complex band at around 1700 cm^{-1} resulting from a carbonyl group (-CHO or -COOH), a band at 2340 cm^{-1} due to adsorbed carbon dioxide CO_2, bands at around 2940 cm^{-1} resulting from C-H stretching modes, a small band at 1640 cm^{-1} due to the bending mode δ(HOH) of adsorbed water, and even a small band at around 1400 cm^{-1}, presumably due to δ(C-H) of some CH_x groups (x = 1, 3 or 3). But the more interesting fact is the evolution of the intensity of the different bands during methanol adsorption. After long accumulation times (25 averaged scans) the EMIR Spectrum

changes greatly (fig.10b) : the intensity of the linearly-bonded CO band increases markedly, whereas the intensity of the other bands decreases drastically. One may conclude that the adsorption of CO removes the other adsorbed species from the electrode surface, explaining thus the difficulty to observe them when the surface is completely blocked by CO.

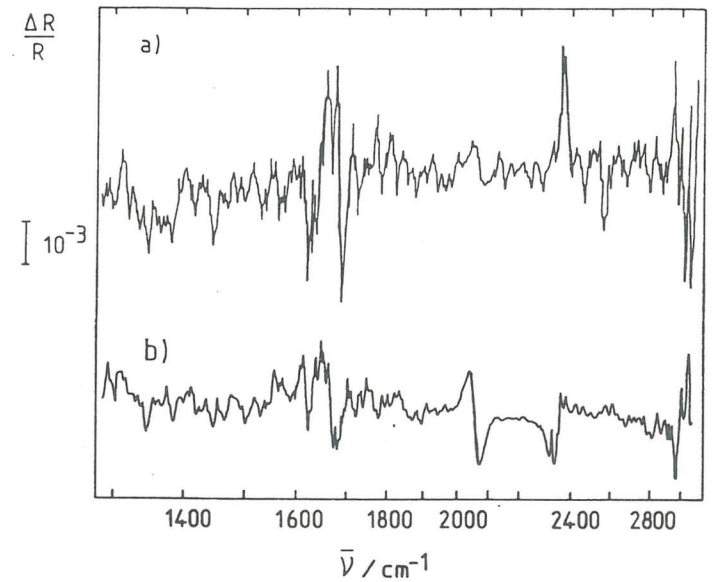

Figure 10 : EMIRS spectra of the species resulting from CH_3OH adsorption at Pt (0.5 M $HClO_4$ + $5x10^{-3}$ M CH_3OH). (a) 1^{st} scan; (b) 25^{th} scan

Similar experiments were realized on rough platinum electrodes (roughness factor $\rho \approx$ 20), which reflect sufficiently the IR light to give EMIR Spectra with a good signal-to-noise ratio (Fig.11). A similar time evolution is observed for a 1 M CH_3OH solution, with an increase of the CO_L band to the expenses of the other banda at around 1700 cm^{-1} (fig.11a). The CO_2 band, due to adsorbed CO_2, is still present, but it changes of sign when the adsorption time increases. But for a 0.1 M CH_3OH solution, the poisoning by adsorbed CO species is greatly reduced (there is only a very weak EMIRS band at around 2060 cm^{-1}), while complex

bands between 1600 and 1700 cm^{-1} still exist at any adsorption time (fig.11b).

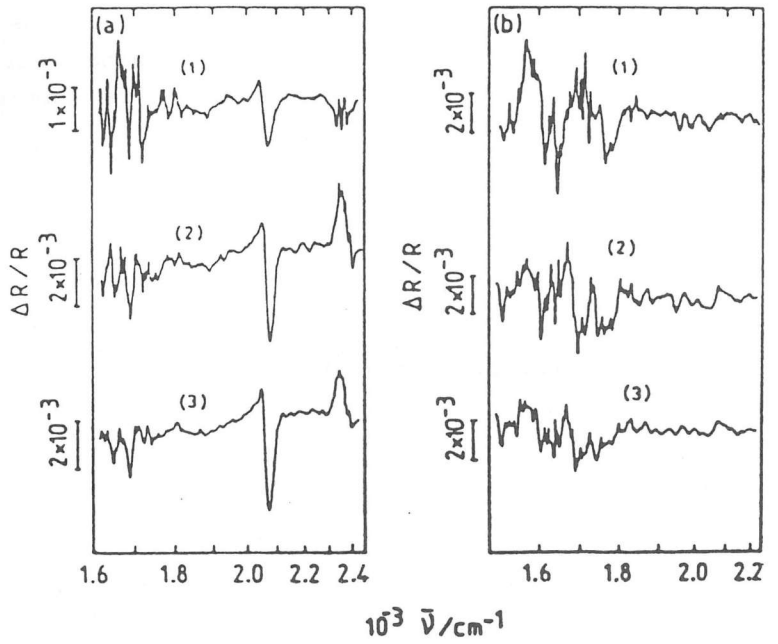

Figure 11 : EMIRS spectra of the adsorbed species from the chemisorption of CH_3OH in 0.5 M $HClO_4$ at a rough Pt electrode. (1)1,(2)5,(3)10 scans; (a) 1 M CH_3OH; (b) 0.1 M CH_3OH

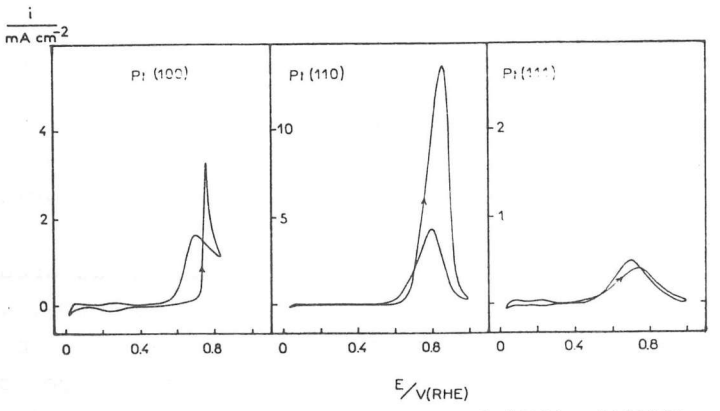

Figure 12 : Voltammograms of Pt(100), Pt(110), Pt(111) single-crystal electrodes in 0.5 M $HClO_4$ + 0.1 M CH_3OH (50 mV/s, 25°C, 1st sweep)

The adsorption and electrooxidation of methanol also

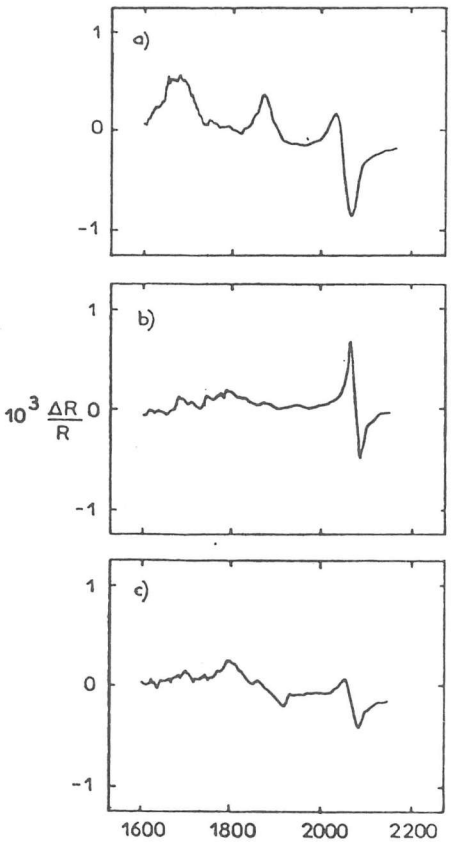

Figure 13 : EMIRS spectra of the adsorbed species resulting from the chemisorption of 0.1 M CH_3OH in 0.5 M $HClO_4$ at Pt(h,k,l) electrodes. a)Pt(100); b)Pt(110); c)Pt(111)

depend greatly on the electrode crystallographic structure, as evidenced by the different intensity vs. potential curves, I(E), obtained by cyclic voltammetry, for the three low index single crystal planes Pt(100), Pt(110) and Pt(111) (fig.12) [18]. EMIRS spectra recorded with the same Pt single crystals under potentiostatic control display similar structural effects : the nature and the distribution of adsorbed species greatly depend on the

electrode structure [18]. Three types of adsorbed intermediates are detected (fig.13) : linearly-bonded -CO at ca. 2070 cm^{-1}, bridge-bonded >CO at ca. 1870 cm^{-1}, and another species at around 1700 cm^{-1}, which may be a formyl-like species, $(-CHO)_{ads}$.

But conversely to polycrystalline Pt, the linearly-bonded CO is not the main adsorbed species, even at high methanol concentrations, except for Pt(110), the behaviour of which is very close to that of polycrystalline platinum. Blocking and poisoning of the platinum catalytic surface, which occurs during the electrooxidation of methanol, were then interpreted in terms of attractive lateral interactions between the different adsorbed CO species.

Finally, the spectroscopic behaviour, together with the electrocatalytic behaviour, of polycrystalline platinum towards methanol oxidation, were computer simulated using the results obtained with the three low index faces. Both the voltammetric curves, I(E), and the EMIRS spectra of polycrystalline Pt, were simulated using the weighted contribution, 15 % Pt(100) + 65 % Pt(110) + 20 % Pt(111), of each single crystal electrode.

(iii) Chemisorption of ethanol at a platinum electrode[19][20]

This example is particularly interesting since ethanol is the first term of the series of aliphatic alcohols with a C-C bond.

It was possible to detect by EMIRS several absorption bands in the range 700-3000 cm^{-1} depending on the electrode potential and on the bulk concentration of ethanol. For low concentrations (e.g. 10^{-3} M), the EMIRS spectrum in the range 1400-3000 cm^{-1} (Fig.14b) displays a main bipolar band at 2070 cm^{-1} (linearly-bonded CO) and a weaker band at around 1850 cm^{-1} (bridge-bonded CO). This proves that chemisorption of ethanol leads to a breaking of the C-C bond, even at room temperature. Another unipolar band at ca. 2350 cm^{-1} is seen, due to adsorbed CO_2 , which may come

from the oxidation of CO. Other bands at around 2880-2980 cm^{-1} are assigned to C-H stretching modes of CH_3 and CH_2 groups. At lower wavenumbers, between 1680 and 1800 cm^{-1} (Fig.14b), several bands due to the stretching mode of carbonyl functional groups are detected, bands which may attributed to acetyl-like or acetaldehyde-like species[19].

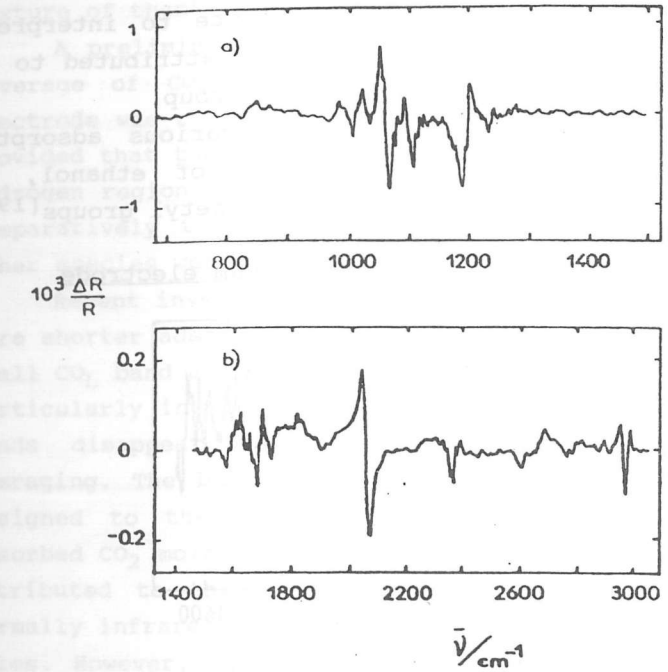

Figure 14 : EMIRS spectra of the adsorbed species resulting from the chemisorption of ethanol in 0.5 M $HClO_4$ at a Pt electrode. a)10^{-1} M, b)10^{-3} M C_2H_5OH

In the wavenumber range 700 to 1400 cm^{-1}, other EMIRS bands are clearly seen for higher ethanol concentrations (fig.14a). The bands between 1000 and 1050 cm^{-1} are due to the stretching mode $\nu(CO)$ of the alcoholic group, whereas a fluctuating band at ca. 1100 cm^{-1} arises from the perchlorate anions.

The early stages of ethanol adsorption at a platinum electrode in acid medium were also investigated. A time dependence, similar to that obtained with methanol, can be observed : the progressive replacement of the weakly

adsorbed species by the CO adsorbed species[20]. But at small adsorption times and low ethanol concentrations, other small bands are also observed at 1200, 1305, 1380, 1620 cm^{-1}. The 1200 cm^{-1} band may be attributed to the C-O stretching mode of an enol-type intermediate, =CHOH, which also gives an IR band at around 3000 cm^{-1} (C-H stretching mode). The other bands are more delicate to interprete, although the band at 1305 cm^{-1} could be attributed to the deformation mode δ(C-H) of a CH_3 or CH_2 group.

These results allow to discuss various adsorption models, including molecular adsorption of ethanol, and adsorption of ethoxy, acetaldehyde, and acetyl groups[19]

(iv) Adsorption of CO_2 at a platinum electrode

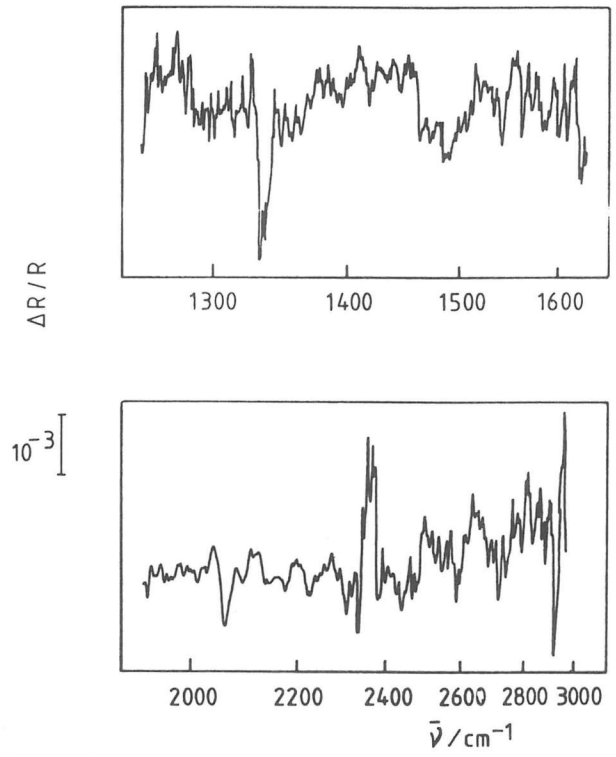

Figure 15 : EMIRS spectra of adsorbed CO_2 at a Pt electrode from a gaseous CO_2 saturated 0.5 M $HClO_4$ solution

Whether CO_2 adsorbs on electrode surfaces, or does not, is an important point, relevant for many aspects of electrocatalysis. In terms of "reduced CO_2" for instance, it was recognized a long time ago that CO_2 could be reduced at Pt electrode surfaces[21], leading to various adsorbed species including -CO, -COOH, ->COH, or, possibly, a mixture of them[22].

A preliminary EMIRS study showed that a nearly full coverage of CO_{ad} species was obtained when a platinum electrode was cycled in a CO_2 gas saturated acid solution, provided that the lowest limit of potential was kept in the hydrogen region[23]. The high contribution of CO_B species, comparatively to CO_L species, was already noted, but no other species were detected.

Recent investigations, still using EMIRS, but at much more shorter adsorption times, enable us to detect, apart a small CO_L band at 2060 cm^{-1}, other bands, two of them being particularly intense at ca. 1335 and 2345 cm^{-1} [24]. These bands disappear by further spectral accumulation and averaging. The band at 2345 cm^{-1} (fig.15) can be readily assigned to the non symmetric vibration of the weakly adsorbed CO_2 molecule, while the one at 1335 cm^{-1} has to be attributed to the symmetric vibration, a mode which is normally infrared inactive according to the usual selection rules. However, assuming that CO_2 is adsorbed by one end (i.e. perpendicular to the surface), the dipole moment of the molecule can interact with the oscillating electric field, and therefore becomes infrared active.

ACKNOWLEDGEMENTS

The authors greatly acknowledge the Committee of the 4th Meeting of the Portuguese Electrochemical Society, particularly Professor A. POMBEIRO, for their kind invitation to participate.

REFERENCES

(1) J. O'M. BOCKRIS and S. SRINIVASAN, Fuel Cells : their Electrochemistry, Mc Graw Hill Book Company, New York (1969).

(2) J. O'M. BOCKRIS, B.E. CONWAY, E. YEAGER and R.R. WHITE, Comprehensive Treatise of Electrochemistry, Vol.3, Electrochemical Energy Conversion and Storage, Plenum Press, New York (1981).

(3) C. LAMY, Electrochim. Acta, 29 (1984) 1581.

(4) A. BEWICK, K. KUNIMATSU, B.S. PONS and J.W. RUSSELL, J. Electroanal. Chem., 160 (1984) 47 .

(5) B. BEDEN and C. LAMY, "Infrared Reflectance Spectroscopy at the electrode electrolyte interface", in "Spectro-electrochemistry - Theory and Practice", R.J. Gale Ed., Plenum Press, New York, (1988) chap.5, p.189.

(6) F. HAHN, B. BEDEN and C. LAMY, J. Electroanal. Chem., 204 (1986) 315.

(7) M. CHOY de MARTINEZ, B. BEDEN, F. HAHN and C. LAMY, J. of Electron Spectroscopy and Related Phenomena, 45 (1987) 153.

(8) M. CHOY de MARTINEZ, B. BEDEN, F. HAHN and C. LAMY, J. Electroanal. Chem, 249 (1988) 265.

(9 R.R. ADZIC, Isr. J. Chem., 18 (1979) 166.

(10) M. CHOY de MARTINEZ, B. BEDEN and C. LAMY, 38th ISE Meeting, Maastricht (The Netherlands), 1987, Extended Abstract 4.66.

(11) B.D. McNICOL, Direct Methanol/Air Systems, in Power Sources for Electric Vehicles, B.D. McNicol and D.A.J. Rand (Eds.), Elsevier, Amsterdam (1984) p.807.

(12) B. BEDEN, A. BEWICK, K. KUNIMATSU and C. LAMY, J. Electroanal. Chem., 121 (1981) 343.

(13) B. BEDEN, F. HAHN, S. JUANTO, C. LAMY and J.M. LEGER, J. Electroanal. Chem., 225 (1987) 215.

(14) K. KUNIMATSU, J. Electroanal. Chem., 140 (1982) 205.

(15) A. BEWICK and S. PONS, in R.J.H. CLARK and R.E. HESTER (Eds.), Advances in Infrared and Raman Spectroscopy, vol.12, Heyden, London (1985) chap.1, p.1.

(16) B. BEDEN, F. HAHN, J.M. LEGER , M.I. DOS SANTOS LOPES and C. LAMY, J. Electroanal. Chem., 258 (1989) 463.

(17) B. BEDEN, F. HAHN, C. LAMY, J.M. LEGER, N.R. de TACCONI, R.O. LEZNA and A.J. ARVIA, J. Electroanal. Chem., in press.

(18) B. BEDEN, S. JUANTO, J.M. LEGER and C. LAMY, J. Electroanal. Chem., 238 (1987) 323.

(19) B. BEDEN, M.C. MORIN, F. HAHN and C. LAMY, J. Electroanal. Chem., 229 (1987) 353.

(20) J.M. PEREZ, B. BEDEN, F. HAHN, A. ALDAZ and C. LAMY, J. Electroanal. Chem., in press.

(21) J. GINER, Electrochim. Acta, 8 (1963) 857 ; 9 (1964) 63.

(22) M.W. BREITER, Electrochim. Acta, 12 (1969) 1213. W. VIELSTICH and V. VOGEL, Z. Elektrochem., 68 (1964) 688.

(23) B. BEDEN, A. BEWICK, M. RAZAQ and J. WEBER, J. Electroanal. Chem., 139 (1982) 203.

(24) J.M. PEREZ, F. HAHN, B. BEDEN and C. LAMY, 4th Meeting of the Portuguese Electrochemical Society, Lisboa (Portugal), March 1989.